

One- and two-magnon excitations in antiferromagnet PbFeBO_4

M. A. Prosnikov^{1,2,*}

1 High Field Magnet Laboratory (HFML - EMFL), Radboud University, Toernooiveld 7,
6525 ED Nijmegen, The Netherlands

2 Radboud University, Institute for Molecules and Materials, Heyendaalseweg 135, 6525 AJ
Nijmegen, The Netherlands

* yotungh@gmail.com

May 29, 2022

Abstract

The linear spin wave theory study of PbFeBO_4 spin dynamics is presented. It is shown that the modes observed in Raman scattering experiments below Néel temperature in [1] are optical magnon and two-magnon excitations. Based on the magnon energy, two-magnon band lineshape, and Weiss temperature [2], the consistent set of the exchange coupling constants up the third neighbor is derived and compared with the results of *ab initio* calculations [3–5]. The small deviation of the observed two-magnon band from the one-magnon density of states suggests a surprisingly negligible role of magnon-magnon interactions.

1 Introduction

The promising field of antiferromagnetic spintronics [6–9] constantly demands the discovery of the new functional materials with specified properties and the development of reliable theoretical models. Some potential material candidates manifest intrinsic coupling of different subsystems such as magnetic, orbital, electronic, and lattice, allowing for additional degrees of freedom to control spin excitations [10–12].

The PbMBO_4 ($\text{M}=\text{Cr}, \text{Mn}, \text{Fe}$) family of compounds belongs to the sillimanite group [13], where the presence of the stereochemically active Pb^{2+} cations leads to the reduction of the connectivity between magnetic ions resulting in the unique topology of the exchange structure [14]. Moreover, the types of magnetic ions drastically affect magnetic properties, such as magnetic structures, critical temperatures, and dispersion of the magnetic excitations without change of crystal symmetry. Notably, PbMnBO_4 is an extremely rare example of insulating ferromagnets [15, 16], while other (PbFeBO_4 and PbCrBO_4) are known to be antiferromagnets [15]. There are a few predicted compounds with other $3d$ ions PbMBO_4 ($\text{M}=\text{Ti}, \text{V}, \text{Co}$) [4], which yet to be synthesized.

In this family, the PbFeBO_4 exhibits the highest transition temperature of $T_N = 114 \text{ K}$, shows anisotropic and negative thermal expansion observed with X-ray and neutron diffraction [17], anomalies in the vicinity of T_N in both dielectric susceptibility [2] and phonon energies [1] indicating coupling between magnetic and lattice subsystems. Magnetostatic and dielectric properties of PbFeBO_4 and PbMnBO_4 were studied in detail in [2, 16]. There are

a number of *ab initio* calculations [3–5, 18] dedicated to the determination of the exchange constants. Simultaneously, the reliable determination of the exchange constants is the crucial step in understanding both the static and dynamical properties of the material and its further potential for applications.

In this paper, we report on the linear spin-wave theory calculations allowing us to derive closed-form magnon dispersion relation for PbFeBO_4 (and equivalent compounds), calculation of the two-magnon (2M) band lineshape, and ground-state phase diagram for exchange couplings up to the third neighbor. The consistent set of the exchange constants (J_0, J_1, J_2) is proposed based on the experimentally observed energy of the optical branch, shape of 2M band [1], and Curie-Weiss temperature [2]. It is shown that both interchain couplings (J_1, J_2) are crucial to capture peculiarities of the spin dynamics. Their values, considering coordination numbers, are comparable with intrachain one the (J_0) classifying PbFeBO_4 as 3D Heisenberg antiferromagnet. The symmetry allowed Dzyaloshinskii-Moriya interaction (DMI) on J_0 path could explain magnetic susceptibility anomaly [2] in the absence of weak ferromagnetic moment and could be directly observed by the zero-field splitting of the acoustical magnon branch. The estimated energy range of magnetic excitations for PbCrBO_4 is briefly discussed at the end.

2 Results and discussion

Below $T_N = 114\text{ K}$ PbFeBO_4 undergoes paramagnetic to antiferromagnetic phase transition with magnetic propagation vector $\mathbf{k} = 0$ according to neutron diffraction measurements [15]. The resulting magnetic structure can be described as coupled antiferromagnetic chains of $[\text{FeO}_6]$ octahedra. Based on exchange interactions up to the third neighbor, the $\mathbf{k} = 0$ ground state phase diagram is calculated through energy minimization [19] and shown in Fig. 1. Two cases of antiferromagnetic and ferromagnetic intrachain interactions were considered, and it is shown that all possible $\mathbf{k} = 0$ magnetic structures could be realized in both cases, however taking into account dominant role of J_0 the most probable structures are AFM2 and AFM1 for $J_0 > 0$ and FM and AFM3 for $J_0 < 0$, respectively.

The following Hamiltonian based on isotropic exchange interactions and single-ion anisotropy (SIA) terms is considered for spin-wave calculations:

$$\mathcal{H} = \sum_{\langle i,j \rangle} J_0 \mathbf{S}_i \mathbf{S}_j + \sum_{\langle\langle i,j \rangle\rangle} J_1 \mathbf{S}_i \mathbf{S}_j + \sum_{\langle\langle\langle i,j \rangle\rangle\rangle} J_2 \mathbf{S}_i \mathbf{S}_j + \sum_i D(\mathbf{S}_i^z)^2, \quad (1)$$

where \mathbf{S} is the spin operator, $J_0..J_2$ stands for superexchange constants corresponding to paths shown in Fig. 1. $J > 0$ corresponds to AFM exchange.

Utilizing Holstein-Primakoff transformations [20] and Fourier transformation of the ex-

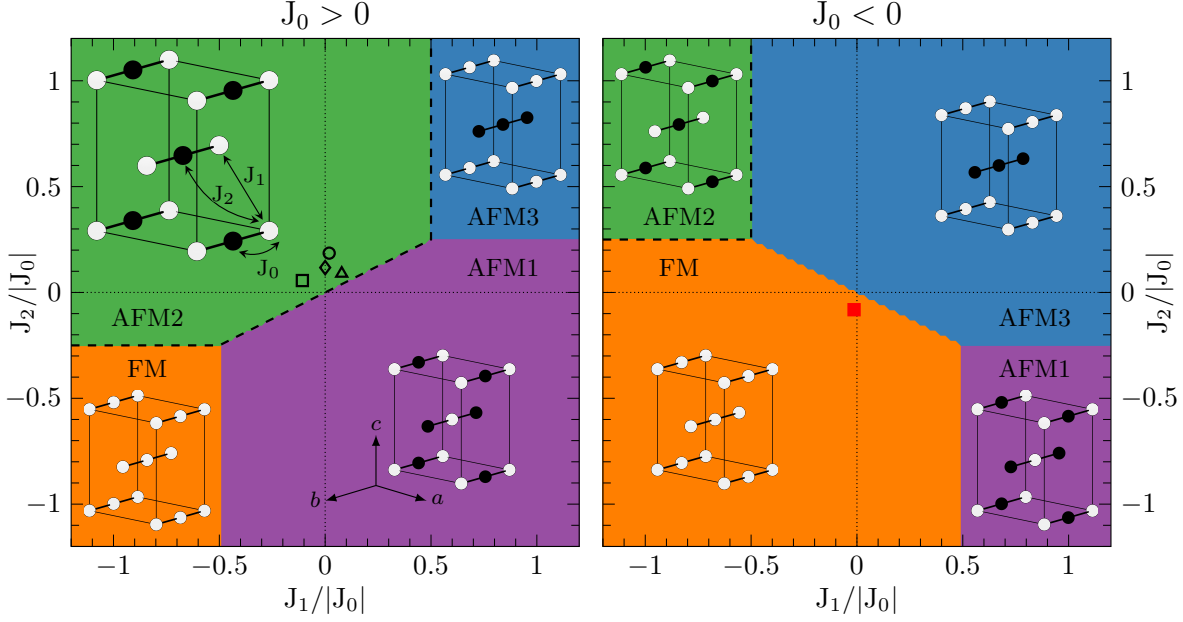


Figure 1: Ground state magnetic phase diagrams as a function of interchain exchange interactions J_1 and J_2 normalized at intrachain one J_0 obtained through energy minimization (colored regions) and according to the real domain of Eq. (4) (thick dashed line). Left and right panels correspond to antiferromagnetic and ferromagnetic intrachain interaction, respectively. Insets depict structures with only magnetic ions shown. Marks shows sets of exchange parameters for PbFeBO_4 calculated in this work (square), Koo et al. [3] (circle), Xiong et al. [4] (triangle), Curti et al. (set b) [5] (diamond), and for PbMnBO_4 Koo et al. [3] (red square).

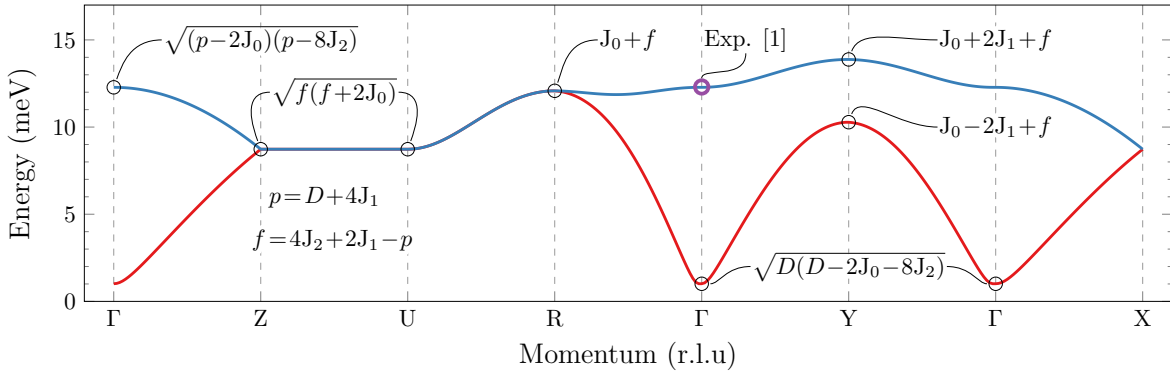


Figure 2: Spin-waves dispersion along the high-symmetry path in the Brillouin zone according to Eq. (4). To obtain the energy of the highlighted points equations should be multiplied by the $2S$ (e.g. $S = 5/2$ for PbFeBO_4). Purple circle shows the energy of the experimentally observed optical branch [1].

change couplings the bosonic matrix form of the Hamiltonian is obtained:

$$\begin{pmatrix} a & b^* & 0 & 0 & 0 & 0 & c^* & e^* \\ b & a & 0 & 0 & 0 & 0 & d & c^* \\ 0 & 0 & a & b^* & c & d^* & 0 & 0 \\ 0 & 0 & b & a & e & c & 0 & 0 \\ 0 & 0 & c^* & e^* & a & b^* & 0 & 0 \\ 0 & 0 & d & c^* & b & a & 0 & 0 \\ c & d^* & 0 & 0 & 0 & 0 & a & b^* \\ e & c & 0 & 0 & 0 & 0 & b & a \end{pmatrix}, \quad (2)$$

where

$$\begin{aligned} a &= 2S (-D + J_0 - 2J_1 + 4J_2), \\ b &= S J_1 \left(1 + e^{2\pi i h}\right) \left(1 + e^{2\pi i l}\right), \\ c &= S J_0 \left(1 + e^{2\pi i k}\right), \\ d &= 8S J_2 \cos(\pi h) \cos(\pi k) \cos(\pi l) e^{\pi i(h-k+l)}, \\ e &= S J_2 \left(1 + e^{2\pi i h}\right) \left(1 + e^{2\pi i k}\right) \left(1 + e^{2\pi i l}\right). \end{aligned} \quad (3)$$

Diagonalization [21] of the matrix leads to two positive doubly-degenerate spin-wave modes corresponding to acoustical and optical branches:

$$\omega = 2 \left[S^2 (\mp 4 \cos(\pi h) \cos(\pi l) (D J_1 + J_1^2 (\mp \cos(\pi h)) \cos(\pi l) + J_0 (J_2 - J_1) + J_0 J_2 \cos(2\pi k) + 2J_1 (J_1 - 2J_2)) + (D - J_0 + 2J_1 - 4J_2)^2 - \cos^2(\pi k) (16J_2^2 \cos^2(\pi h) \cos^2(\pi l) + J_0^2)) \right]^{1/2}, \quad (4)$$

where h, k, l are given in reciprocal lattice units, and different branches are distinguished by \mp sign. Obtained dispersion curves and surfaces are shown in Fig. 2 and Fig. 3, respectively.

All the calculations and plots were done with a small value of the single ion easy-axis type anisotropy of -0.01 meV (along the c axis) to reproduce the observed magnetic structure of PbFeBO_4 [15]. Despite the fact that it is impossible to derive the precise value of SIA based on the existing experimental data, which will require the frequency of the acoustical magnon, it is possible to estimate its boundaries. No acoustical modes were observed above $10 \text{ cm}^{-1} \approx 1.24 \text{ meV}$ according to [1], thus it can be used to estimate a higher boundary of SIA. The lower one could be estimated by taking into account the absence of acoustic mode up to $140 \text{ GHz} \approx 4.17 \text{ cm}^{-1} \approx 0.58 \text{ meV}$ in antiferromagnetic resonance (AFMR) experiments [2]. Thus using the set of the exchange constants from Table 1 and with Eq. (4) will get anisotropy bounds of $-0.015 < D < -0.0033 \text{ meV}$. The validity of the obtained analytical results was confirmed by numerical calculations with SpinW library [19, 22].

2.1 Two-magnon scattering

The most prominent feature observed in the magnetic Raman scattering spectra [1] below T_N is the broad and complex-shaped band attributed to the two-magnon scattering process due to its spectral and temperature-dependent characteristics. First, we will start with the

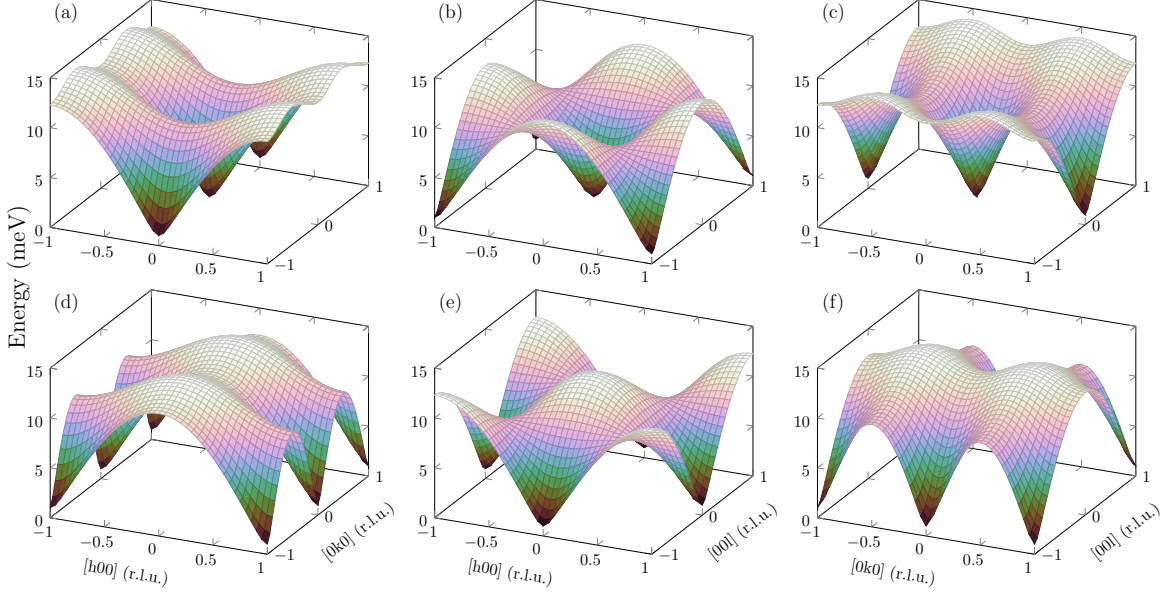


Figure 3: Spin-wave dispersion for PbFeBO_4 given by Eq. (4) with exchange coupling constants from the first row of Table 1.

selection rules. The effective two-magnon Raman Hamiltonian can be written according to the exchange scattering Fleury-Loudon mechanism [23]:

$$\mathcal{H}_R \propto \sum_{i,d} (\mathbf{e}_I \cdot \mathbf{d})(\mathbf{e}_S \cdot \mathbf{d}) \mathbf{S}_i \mathbf{S}_j, \quad (5)$$

where \mathbf{e}_I and \mathbf{e}_S denote the polarization vectors of the incident and scattered light, and \mathbf{d} is the vector connecting i -th ion with its nearest-neighbor for the specific exchange coupling. Thus, taking into account only dominant intrachain J_0 interaction, this analysis predicts nonzero two-magnon scattering intensity only in (bb) polarizations, the case where both incident and scattered light polarized along the chains, which was, indeed, observed in the experiment [1].

It is known that two-magnon excitations observed, e.g., by Raman scattering, reflect the spin-wave density of states (DOS) [23], which can be directly calculated based on dispersion relations Eq. (4). It is necessary to use the full form of Hamiltonian Eq. (1) including all the exchange interactions to calculate the energy-depended shape of the two-magnon band, since they drastically affect the shape of the band. Density of states is calculated according to:

$$DOS = \oint_{E(x,y,z)=\epsilon} \frac{dS}{|\nabla E(x,y,z)|}, \quad (6)$$

where integral is taken numerically through constant energy surfaces within the first Brillouin zone. The results of the calculations for different sets of exchange couplings from Table 1 in comparison with the experiment are shown in Fig. 4.

This approach, along with a proposed set of the optimized exchange constants $J_0 = 1.67$, $J_1 = -0.18$, $J_2 = 0.094$ meV allowed us to capture all essential experimental observations [1] such as (i) high energy cut-off of the band at 28 meV (ii) characteristic curvature

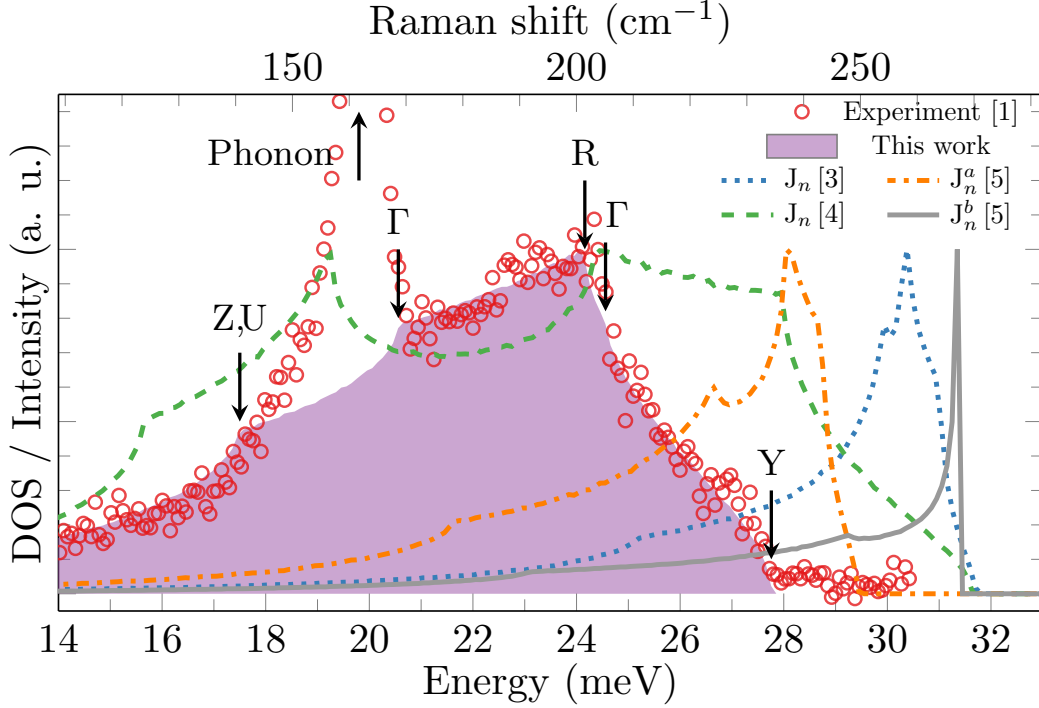


Figure 4: Comparison of experimental Raman scattering spectra of two-magnon band (red marks, data extracted from Fig. 5 in [1]) with the spin-wave density of states calculated with exchange constants from [3–5]. Note that DOS energy scale is doubled to match 2M excitation. Arrows indicate Van Hove singularities in DOS with corresponding critical points in the Brillouin zone.

of the band in the 24–28 meV range (iii) nearly linear DOS of maximal energy in within 21–24 meV (iv) nonzero and non-linear low-energy tail for energies less than 18 meV.

The limiting factors of further refinement of the exchange constants using 2M band are the presence of the intense phonon with the same A_g symmetry with the energy of ≈ 19.5 meV, overshadowing part of the expected singularities, a rather noisy spectrum, and the absence of quantitative information on the lower energy tail.

It should be noted that one-magnon DOS surprisingly well describes the experimentally observed two-magnon band. Usually, it is apparently different due to the magnon-magnon interactions [24] that strongly dampen and shift such excitations, which was demonstrated in paradigmatic examples of NiO [25] and RbMnF₃ [26]. The negligible role of the magnon-magnon interactions could mean an increased lifetime of spin excitations [27], which is a highly desirable goal for practical applications in antiferromagnetic spintronics [6]. An interesting aspect is the presence of the pronounced Van Hove singularities in the 2M band, which can provide access to magnons in the specific points in the Brillouin zone and could be potentially applied to modulate exchange interactions and to control magnetic order in ultrafast timescales [28, 29]. Another striking feature is the accidental degeneracy of the high-energy (12.4 meV) optical magnon branch with A_g phonon in the low-temperature limit, which could be used for spin dynamics manipulation through optical phonon pumping [30].

2.2 Comparison with *ab initio* calculations

Realization of both ferromagnetic and antiferromagnetic structures for different magnetic ions without change of the crystal symmetry in PbMBO_4 ($M=\text{Cr, Mn, Fe}$) family spark the interest, and a few computational works [3–5] were done to shed light on this phenomenon. Lattice dynamics was addressed in [5, 17] and, in general, shows a good match with experimental data both on powdered samples [17] and single crystals [1].

Exchange constants up to the third neighbor were directly calculated in [3, 5] and, using energy mapping analysis (Eq. 3 in [3]), it is possible to extract constants from the energies of the magnetic structures from [4], which all summarized in Table 1 and graphically shown in Fig. 1. All calculations agree on the dominant role of the intrachain exchange (J_0). The J_1 is either antiferromagnetic or zero in the case of Gibbs free energy calculations [5] and smaller than J_2 , which is also antiferromagnetic. It was shown that exchange constants are strongly dependent on Hubbard parameter U in DFT+ U scheme [3]. The comparison of the sets, with the experimental 2M band presented in Fig. 4, clearly showing interchain coupling sensitivity, and substantial deviation for all the *ab initio* sets.

Besides the direct determination of the exchange constants based on one- and two-magnon excitations, it is possible to use static magnetic data as an additional consistency check. For example, Curie-Weiss temperature (sometimes referred to as Weiss or paramagnetic Curie temperature), which is the arithmetic average of all the exchange constants in the system [31], could be used. Taking into account the number and symmetry of the exchange couplings, it can be calculated as:

$$\Theta = -\frac{2}{3}S(S+1)[2J_0 + 4J_1 + 8J_2]/k_B . \quad (7)$$

This parameter could be experimentally determined from the temperature dependence of the magnetic susceptibility for $T > T_N$. This was done experimentally [2], and the reported values are negative, suggesting predominantly antiferromagnetic interactions in the system, and slightly anisotropic $\Theta_a = -256$, $\Theta_b = -272$, $\Theta_c = -262$ K. Most of the sets, proposed in *ab initio* works [3–5] overestimate Θ by 54–81 %. In contrast the optimal set of the exchange constants results in much closer value $\Theta = -228$ K. The deviation of Θ from the proposed set could be explained by additional unaccounted superexchange couplings beyond J_2 or by the contribution of non-isotropic exchange interactions (see Section 2.3).

The calculated exchange parameters in comparison with previously suggested ones are summarized in Table 1. We hope that the proposed set of exchange constants, compatible with all up to date experimental observations, will be used for a systematic search of U parameter in such a challenging system as PbFeBO_4 .

2.3 Beyond isotropic exchange

The unexplained anomaly was reported in [2], where unusual for typical easy-axis antiferromagnet peak-like maximum in the magnetic susceptibility for $H \parallel b$ geometry was measured. Thus the potential presence of the anisotropic exchange couplings terms, such as Dzyaloshinskii-Moriya interaction, should be discussed. In most cases, such interaction leads to a spin canting resulting in similar anomalies in susceptibility and a presence of the weak macroscopic magnetic moment in antiferromagnets [32, 33], like in some well-known cases such as FeBO_3 [34], LiCoPO_4 [35], perovskite manganites [36], etc. However, no magnetic moment was registered in PbFeBO_4 for all the available field ranges and geometries [2].

	J_0	J_1	J_2	OM_{calc}	OM_{exp}	Θ_{calc}	Θ_{exp}
This work	1.67	-0.18	0.094	12.28	—	-228	—
Koo <i>et al.</i> [3]	1.81	0.03447	0.3361	14.95	—	-436	—
Xiang <i>et al.</i> [4]	2.321	0.1815	0.20775	9.64	—	-476	—
Curti <i>et al.</i> [5] ²	1.896	0.03447	0.259	13.35	—	-406	—
Curti <i>et al.</i> [5] ³	2.1285	0.0	0.2499	14.64	—	-423	—
Pankrats <i>et al.</i> [2]	—	—	—	—	—	—	-263 ¹
Park <i>et al.</i> [15]	2.24	—	—	11.2	—	-303	—
Prosnikov <i>et al.</i> [1]	2.23	—	—	11.15	12.4	—	—

¹Averaged value, anisotropic ones are $\Theta_a = -256$ K, $\Theta_b = -272$ K, $\Theta_c = -262$ K [2]

^{2,3}For only electronic energy and additional terms, respectively. For the details see Table 1 in [5].

Table 1: Comparison of the exchange constants (meV, $J > 0$ corresponds to AFM) and derived parameters, such as energies of the optical magnon branch (OM, meV, calculated according to Eq. (4)), and Weiss temperatures Θ_{calc} (K, calculated according to Eq. (7)).

It is known that DMI is governed by lattice symmetry [32]. Due to the presence of a mirror plane (m) perpendicular to the J_0 exchange path and passing through its center, only $[DM_x, 0, DM_z]$ components of the DMI vector are allowed. The DM_x will lead to a slight canting of the spins within bc -planes inducing small ferromagnetic moment along individual chains. However, due to the symmetry of the lattice, this canting is compensated by the same moment with the opposite direction from neighboring chains. This canting is fully compatible with previously suggested magnetic space group $Pnma$ [1] and can be described with Ψ_x basis function. On the other hand, the contribution of the DM_z is negligible due to the orientation of the magnetic moments along the same axis.

Thus, the contribution of the antisymmetric exchange interaction with the DM_x component can simultaneously explain the kink-like anomaly in magnetic susceptibility for $H \parallel b$ at T_N and the absence of weak ferromagnetic moment at lower temperatures. This interaction will also directly affect spin dynamics in the form of magnon degeneracy lifting even without external magnetic field presence. Numerical estimation of the acoustic mode splitting by the DMI with the semi-arbitrary value of 0.167 meV (1/10 of J_0) leads to $2.46 \text{ cm}^{-1} \approx 0.3 \text{ meV}$ splitting of the acoustic mode which should be experimentally detectable with reasonably high-resolution Raman or IR spectroscopy setups.

2.4 Magnetic structure dimensionality

The assumption of the (quasi) one-dimensional (1D) magnetism in PbFeBO_4 comes naturally considering its crystal structure, consistent from the well-separated chains of $[\text{FeO}_6]$ octahedra running along the b -axis [15]. The broad features above T_N in dc magnetic susceptibility on powdered samples [15] was also considered as a manifestation of short-range ordering characteristic for low-dimensional magnetic systems. However, the detailed susceptibility investigation on the high-quality single crystals [2] showed that broad features were caused by $\alpha\text{-Fe}_2\text{O}_3$ contamination, and χ behaves closer to three-dimensional Heisenberg antiferromagnet (except kink anomaly which was discussed in Section 2.3).

As the magnetic dimensionality measure, ratios of the intra- to interchain exchange couplings, taking into account coordination number (z_n), could be used [37]. The set of the optimal constants gives following values: $1 : 0.22 : 0.22$ of $|J|_0 * z_0 : |J|_1 * z_1 : |J|_2 * z_2$

which is closer to a 3D case, in comparison with other well-known one-dimensional systems as TTF-CuBDT [38], CuGeO₃ [39], and KCuF₃ [40] with ratios $J_{intra}/J_{inter} \ll 1$. Moreover, in most 1D systems, only single interchain coupling (nnn) is considered important, while for PbFeBO₄, both nnn and $nnnn$ couplings are equally strong.

Thus, based on the above, PbFeBO₄ should be considered a three-dimensional antiferromagnet in the low-temperature limit $T \ll T_N$. However, according to the magnetic susceptibility anomaly observed in [2] and intense magnetic quasi-elastic scattering observed in polarization along the chains [1], there is a possibility of quasi-one-dimensional behavior manifestation in the vicinity of the phase transition.

2.5 Spin dynamics of PbCrBO₄

In comparison with PbFeBO₄, the magnetic structure of PbCrBO₄ differs only in the direction of the easy axis [15]; thus, all previously derived equations and conclusions could be directly applied for an estimation of the energy of one- and two-magnon excitations. Considering more than one order of magnitude lower $T_N = 8$ K, and $\Theta = 45$ K, the exchange constants are expected to be proportionally smaller. However, up to now, there are no published data on the spin dynamics of PbCrBO₄.

According to [3] the exchange parameters of the optimized structure (calculated with Hubbard parameter $U = 2.0$ eV) are $J_0 \approx 0.52$ meV, $J_1 \approx -0.0345$ meV, and $J_2 \approx 0.069$ meV, which with reduced, in comparison with PbFeBO₄, the spin value of Cr³⁺ ions $S = 3/2$ gives expected energy of two-magnon excitation band maximum of ≈ 5 meV and the energy of optical magnon mode at ≈ 2.7 meV which are both accessible in typical low-energy Raman scattering experiments.

3 Conclusion

With the use of linear spin-wave theory, the closed-form of the magnon dispersion relation of PbFeBO₄ was derived, including exchange couplings up to the third neighbor and single-ion anisotropy of the easy axis type. It is demonstrated that magnetic excitations observed in Raman scattering [1] are optical (exchange) magnon and two-magnon band and based on their energy and magnetic susceptibility data [2], the consistent set of exchange coupling constants is proposed: $J_0 = 1.67$, $J_1 = -0.18$, $J_2 = 0.094$ meV. It is shown that *ab initio* calculations [3–5] overestimate both J_0 and J_2 while predicts the opposite sign for J_1 . Nonzero components of the Dzyaloshinskii-Moriya interaction are allowed for the J_0 exchange path, which could be responsible for the magnetic susceptibility anomaly [2]. Surprisingly, the shape of the two-magnon band is well described by the one-magnon density of states, which indicates a vanishingly small role of the magnon-magnon interactions. We hope that obtained results will stimulate both experimental research, such as IR and low-energy Raman spectroscopy to find acoustic modes and inelastic neutron scattering to directly probe magnon dispersion, and theoretical ones on spin dynamics and a systematic study of the exchange coupling constants dependence of Hubbard parameter (U) for *ab initio* calculations.

Acknowledgements

The support of A. M. Kalashnikova, fruitful discussions with Beatrice T. Crow, and assistance with the carbon tube by M. Berben are greatly acknowledged. We also acknowledge the support of the HFML-RU/NWO-I, member of the European Magnetic Field Laboratory (EMFL).

References

- [1] M. A. Prosnikov, A. N. Smirnov, V. Y. Davydov, K. A. Sablina and R. V. Pisarev, *Lattice and magnetic dynamics of a quasi-one-dimensional chain antiferromagnet PbFeBO₄*, Journal of Physics: Condensed Matter **29**(2), 025808 (2016), doi:10.1088/0953-8984/29/2/025808.
- [2] A. Pankrats, K. Sablina, D. Velikanov, A. Vorotynov, O. Bayukov, A. Eremin, M. Molochev, S. Popkov and A. Krasikov, *Magnetic and dielectric properties of the PbFeBO₄ single crystal*, Journal of Magnetism and Magnetic Materials **353**, 23 (2014), doi:10.1016/j.jmmm.2013.10.018.
- [3] H.-J. Koo and M.-H. Whangbo, *Density functional investigation of the magnetic properties of PbMBO₄ (M= Cr, Mn, Fe)*, Solid State Communications **149**(15-16), 602 (2009), doi:10.1016/j.ssc.2009.01.030.
- [4] H. Xiang, Y. Tang, S. Zhang and Z. He, *Intra-chain superexchange couplings in quasi-1D 3d transition-metal magnetic compounds*, Journal of Physics: Condensed Matter **28**(27), 276003 (2016), doi:10.1088/0953-8984/28/27/276003.
- [5] M. Curti, M. M. Murshed, T. Bredow, D. W. Bahnemann, T. M. Gesing and C. B. Mendive, *Elastic, phononic, magnetic and electronic properties of quasi-one-dimensional PbFeBO₄*, Journal of Materials Science (2019), doi:10.1007/s10853-019-03866-1.
- [6] P. Němec, M. Fiebig, T. Kampfrath and A. V. Kimel, *Antiferromagnetic opto-spintronics*, Nature Physics **14**(3), 229 (2018), doi:10.1038/s41567-018-0051-x.
- [7] E. V. Gomonay and V. M. Loktev, *Spintronics of antiferromagnetic systems*, Low Temperature Physics **40**(1), 17 (2014), doi:10.1063/1.4862467.
- [8] V. Baltz, A. Manchon, M. Tsoi, T. Moriyama, T. Ono and Y. Tserkovnyak, *Antiferromagnetic spintronics*, Reviews of Modern Physics **90**(1), 015005 (2018), doi:10.1103/revmodphys.90.015005.
- [9] T. Jungwirth, X. Marti, P. Wadley and J. Wunderlich, *Antiferromagnetic spintronics*, Nature Nanotechnology **11**(3), 231 (2016), doi:10.1038/nnano.2016.18.
- [10] N. A. Spaldin and R. Ramesh, *Advances in magnetoelectric multiferroics*, Nature Materials **18**(3), 203 (2019), doi:10.1038/s41563-018-0275-2.

- [11] J. Son, B. C. Park, C. H. Kim, H. Cho, S. Y. Kim, L. J. Sandilands, C. Sohn, J.-G. Park, S. J. Moon and T. W. Noh, *Unconventional spin-phonon coupling via the Dzyaloshinskii–Moriya interaction*, npj Quantum Materials **4**(1), 1 (2019), doi:10.1038/s41535-019-0157-0.
- [12] S. Han, J. Lee and E.-G. Moon, *Lattice vibration as a knob for novel quantum criticality: Emergence of supersymmetry from spin-lattice coupling*, arXiv:1911.01435 [cond-mat, physics:hep-th] (2019), ArXiv: 1911.01435.
- [13] R. X. Fischer and H. Schneider, *Crystal chemistry of borates and borosilicates with mullite-type structures: a review*, European Journal of Mineralogy **20**(5), 917 (2008), doi:10.1127/0935-1221/2008/0020-1831.
- [14] M. M. Murshed, R. X. Fischer and T. M. Gesing, *The role of the Pb^{2+} lone electron pair for bond valence sum analysis in mullite-type $PbMBO_4$ ($M = Al, Mn$ and Fe) compounds*, Zeitschrift für Kristallographie - Crystalline Materials **227**(8), 580 (2012), doi:10.1524/zkri.2012.1483.
- [15] H. Park, R. Lam, J. E. Greedan and J. Barbier, *Synthesis, Crystal Structure, Crystal Chemistry, and Magnetic Properties of $PbMBO_4$ ($M = Cr, Mn, Fe$): A New Structure Type Exhibiting One-Dimensional Magnetism*, Chemistry of Materials **15**(8), 1703 (2003), doi:10.1021/cm0217452.
- [16] A. Pankrats, K. Sablina, M. Eremin, A. Balaev, M. Kolkov, V. Tugarinov and A. Bovina, *Ferromagnetism and strong magnetic anisotropy of the $PbMnBO_4$ orthoborate single crystals*, Journal of Magnetism and Magnetic Materials **414**, 82 (2016), doi:10.1016/j.jmmm.2016.04.042.
- [17] M. M. Murshed, C. B. Mendive, M. Curti, G. Nénert, P. E. Kalita, K. Lipinska, A. L. Cornelius, A. Huq and T. M. Gesing, *Anisotropic lattice thermal expansion of $PbFeBO_4$: A study by X-ray and neutron diffraction, Raman spectroscopy and DFT calculations*, Materials Research Bulletin **59**, 170 (2014), doi:10.1016/j.materresbull.2014.07.005.
- [18] M. Curti, C. B. Mendive, T. Bredow, M. M. Murshed and T. M. Gesing, *Structural, vibrational and electronic properties of $SnMBO_4$ ($M = Al, Ga$): a predictive hybrid DFT study*, Journal of Physics: Condensed Matter **31**(34), 345701 (2019), doi:10.1088/1361-648X/ab20a1.
- [19] S. Tóth, *tsdev/spinw: pyspinw 3.0*, doi:10.5281/zenodo.838034 (2017).
- [20] T. Holstein and H. Primakoff, *Field Dependence of the Intrinsic Domain Magnetization of a Ferromagnet*, Physical Review **58**(12), 1098 (1940), doi:10.1103/PhysRev.58.1098.
- [21] R. M. White, M. Sparks and I. Ortenburger, *Diagonalization of the Antiferromagnetic Magnon-Phonon Interaction*, Physical Review **139**(2A), A450 (1965), doi:10.1103/PhysRev.139.A450.
- [22] S. Toth and B. Lake, *Linear spin wave theory for single- Q incommensurate magnetic structures*, Journal of Physics: Condensed Matter **27**(16), 166002 (2015), doi:10.1088/0953-8984/27/16/166002.

- [23] P. A. Fleury and R. Loudon, *Scattering of Light by One- and Two-Magnon Excitations*, Physical Review **166**(2), 514 (1968), doi:10.1103/PhysRev.166.514.
- [24] R. J. Elliott and M. F. Thorpe, *The effects of magnon-magnon interaction on the two-magnon spectra of antiferromagnets*, Journal of Physics C: Solid State Physics **2**(9), 1630 (1969), doi:10.1088/0022-3719/2/9/312.
- [25] R. E. Dietz, G. I. Parisot and A. E. Meixner, *Infrared Absorption and Raman Scattering by Two-Magnon Processes in NiO*, Physical Review B **4**(7), 2302 (1971), doi:10.1103/PhysRevB.4.2302.
- [26] P. A. Fleury, *Evidence for Magnon-Magnon Interactions in RbMnF₃*, Physical Review Letters **21**(3), 151 (1968), doi:10.1103/PhysRevLett.21.151.
- [27] M. E. Zhitomirsky and A. L. Chernyshev, *Colloquium: Spontaneous magnon decays*, Reviews of Modern Physics **85**(1), 219 (2013), doi:10.1103/RevModPhys.85.219.
- [28] J. H. Mentink, *Manipulating magnetism by ultrafast control of the exchange interaction*, Journal of Physics: Condensed Matter **29**(45), 453001 (2017), doi:10.1088/1361-648X/aa8abf.
- [29] G. Batignani, D. Bossini, N. Di Palo, C. Ferrante, E. Pontecorvo, G. Cerullo, A. Kimel and T. Scopigno, *Probing ultrafast photo-induced dynamics of the exchange energy in a Heisenberg antiferromagnet*, Nature Photonics **9**(8), 506 (2015), doi:10.1038/nphoton.2015.121.
- [30] T. F. Nova, A. Cartella, A. Cantaluppi, M. Först, D. Bossini, R. V. Mikhaylovskiy, A. V. Kimel, R. Merlin and A. Cavalleri, *An effective magnetic field from optically driven phonons*, Nature Physics **13**(2), 132 (2017), doi:10.1038/nphys3925.
- [31] A. Czachor, *Paramagnetic Curie temperature is an arithmetic average of the interspin coupling constants*, Journal of Magnetism and Magnetic Materials **139**(3), 355 (1995), doi:10.1016/0304-8853(95)90014-4.
- [32] T. Moriya, *Anisotropic Superexchange Interaction and Weak Ferromagnetism*, Physical Review **120**(1), 91 (1960), doi:10.1103/PhysRev.120.91.
- [33] A. Moskvin, *Dzyaloshinskii–Moriya Coupling in 3d Insulators*, Condensed Matter **4**(4), 84 (2019), doi:10.3390/condmat4040084.
- [34] V. E. Dmitrienko, E. N. Ovchinnikova, S. P. Collins, G. Nisbet, G. Beutier, Y. O. Kvashnin, V. V. Mazurenko, A. I. Lichtenstein and M. I. Katsnelson, *Measuring the Dzyaloshinskii–Moriya interaction in a weak ferromagnet*, Nature Physics **10**(3), 202 (2014), doi:10.1038/nphys2859.
- [35] E. Fogh, O. Zaharko, J. Schefer, C. Niedermayer, S. Holm-Dahlin, M. K. Sørensen, A. B. Kristensen, N. H. Andersen, D. Vaknin, N. B. Christensen and R. Toft-Petersen, *Dzyaloshinskii–Moriya interaction and the magnetic ground state in magnetoelectric LiCoPO₄*, Physical Review B **99**(10), 104421 (2019), doi:10.1103/PhysRevB.99.104421.

- [36] I. A. Sergienko and E. Dagotto, *Role of the Dzyaloshinskii-Moriya interaction in multiferroic perovskites*, Physical Review B **73**(9), 094434 (2006), doi:10.1103/PhysRevB.73.094434.
- [37] P. Lemmens, G. Güntherodt and C. Gros, *Magnetic light scattering in low-dimensional quantum spin systems*, Physics Reports **375**(1), 1 (2003), doi:10.1016/S0370-1573(02)00321-6.
- [38] C. Jeandey and M. Nechtschein, *Inter- and intra-chain couplings in TTF CuBDT as determined from proton spin lattice relaxation time measurements*, Journal of Magnetism and Magnetic Materials **15-18**, 1053 (1980), doi:10.1016/0304-8853(80)90884-7.
- [39] M. Nishi, O. Fujita and J. Akimitsu, *Neutron-scattering study on the spin-Peierls transition in a quasi-one-dimensional magnet CuGeO₃*, Physical Review B **50**(9), 6508 (1994), doi:10.1103/PhysRevB.50.6508.
- [40] K. Hirakawa and Y. Kurogi, *One-Dimensional Antiferromagnetic Properties of KCuF₃*, Progress of Theoretical Physics Supplement **46**, 147 (1970), doi:10.1143/PTPS.46.147.